FISEVIER

Contents lists available at ScienceDirect

Analytica Chimica Acta

journal homepage: www.elsevier.com/locate/aca



Electrokinetic stacking of particle zones in confined channels enabling their UV absorbance detection on microchips



Ling Xia, Rajesh Deb, Debashis Dutta*

Department of Chemistry, University of Wyoming, Laramie, WY, 82071, USA

HIGHLIGHTS

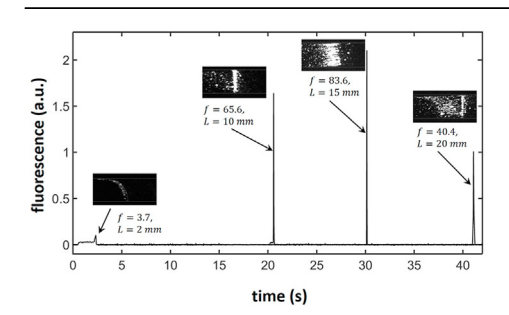
- Particle zones were focused by electroosmotically driving them in glass channels.
- Sample peaks were focused by over 2 orders of magnitudes for polystyrene beads.
- Sample quantitation was demonstrated based on the area of the sample peak.
- UV detection of polystyrene particles was enabled in a 5 μm deep quartz channel.
- The reported method allowed successful estimation of colloidal content in natural water samples.

ARTICLE INFO

Article history:
Received 23 March 2020
Received in revised form
6 August 2020
Accepted 10 August 2020
Available online 22 August 2020

Keywords:
Electrokinetic injection
Electroosmosis
Microfluidics
Micro-/nanoparticles
Pre-concentration
UV absorbance detection

G R A P H I C A L A B S T R A C T



ABSTRACT

In this article, we report a simple approach to stacking micro- and nanoparticle zones by electrokinetically migrating them through moderately confined channels of uniform cross-section. Experiments show the reported pre-concentration process to initiate at the tail end of the zone following its electrokinetic injection, with the stacked region migrating faster than the rest of the sample band. This effect causes the particles traveling in front to merge into the stacked region making it grow both in size and concentration. Because the stacked zone also gradually loses particles from its trailing edge, it eventually disintegrates upon running out of particles at its front end. Nevertheless, enhancements in peak height by over 100-fold were recorded using the reported approach for polystyrene beads with diameters comparable to the channel depth. This enhancement however, exhibited a temporal variation as the particle band migrated through the analysis column reaching a maximum value that depended on the particle diameter, particle concentration, channel depth, electric field strength, electroosmotic mobility, etc. Interestingly, the peak area recorded by the detector remained relatively constant during this particle migration period allowing reliable sample quantitation. Moreover, upon incubating antibody-coated particles against an antigen sample, the peak area for the particle zone was seen to scale linearly with the antigen concentration establishing the utility of the reported focusing phenomenon for chemical/ biochemical analysis. The noted stacking technique was further applied to enabling UV absorbance detection of particle zones on microchips which then allowed us to determine the colloidal content in actual natural water samples. .

© 2020 Elsevier B.V. All rights reserved.

E-mail address: ddutta@uwyo.edu (D. Dutta).

^{*} Corresponding author.

1. Introduction

Micro- (microfluidic) and sub-micrometer (nanofluidic) scale channels offer a powerful platform for miniaturizing traditional analytical methods yielding performances superior to their macroscopic and capillary-based counterparts in several applications [1-3]. Moreover, the strong interaction of the analyte molecules/particles with the channel surface in these systems promises the development of unique assays which can significantly advance our scientific capabilities [4,5]. Unfortunately however, the shorter optical path length in these conduits can pose a significant challenge to allowing reliable detection of sample molecules/particles during the analysis procedures. As a result, there has been a major emphasis towards developing and integrating sample preconcentration methods to micro-/nanofluidic assays since the inception of the lab-on-a-chip platform [6-8]. More recently, sample pre-concentration approaches have been also integrated to paper-based analytical devices that are typically known to yield limited detection sensitivities owing to their simplistic nature [9,10]. A majority of microchip based pre-concentration techniques reported in the literature though, have been designed for trapping molecular species within the detection region. Among these, sample stacking strategies based on the use of electric fields around membranes [11-14], micro-/nanochannel interfaces [15,16] and liquid-liquid junctions [17,18] have been of most interest to the research community due to their ease of implementation at the micro-/sub-micrometer length scale. It must be noted that although approaches involving the capture of analyte molecules onto a target surface [19] or their extraction into a desired solvent [20] offer useful alternatives to realizing sample stacking, they are not always as readily integrable to various microchip operations as the electric field based methods referenced above.

The use of electrical forces for maneuvering larger entities such as biological cells and colloidal particles within microfluidic networks have also proven effective in a variety of applications [21,22]. In this regard, dielectrophoretic techniques have gained the most attention primarily due to their ability to simultaneously separate and accumulate cells/particles in a high throughput fashion [23,24]. The use of electric field for depositing particles over electrode surfaces has been demonstrated to be another approach of considerable technological promise that can allow the realization of colloidal patterns over relatively large areas [25,26]. It must be pointed out however, that in spite of the developments described above, the accuracy and precision with which the transport of colloidal particles can be controlled within microchannels using electric fields is often not as high as in the case of molecular species. A major reason for this limitation is the finite size of the particles which tends to distort the field lines in their vicinity. Moreover, differences in material properties, e.g., dielectric constant, between the colloidal and the continuous phases have been shown to generate secondary flows that can affect particle migration and dispersion [27,28]. Nevertheless, the rich electrohydrodynamic phenomena driving particle motion under the influence of an electric field in micro-/nanochannels offer plentiful opportunities for designing unique assays that have not been explored yet.

In this article, we report one such phenomenon that allows the stacking of particle zones during their electroosmotic migration through a channel of uniform cross-section. Our experiments show that when a zone of colloidal particles is electrokinetically introduced into an analysis duct using the gated injection scheme, a small stacked region of these entities is formed at the tail end of the band.

Interestingly, this region is noticed to migrate somewhat faster than the particles traveling in front causing them to merge into the stacked zone making it grow in size and concentration. Enhancements in peak height by over 2 orders of magnitude were realized using this approach for polystyrene beads with diameters comparable to the channel depth. The noted enhancement however, exhibited a temporal variation as the particle band migrated through the analysis column and went through a maximum value that depended on several parameters such as particle diameter, particle concentration, channel depth, electric field strength, electroosmotic mobility, etc., in the system. Interestingly, the area under the sample peak remained relatively constant in these measurements which allowed reliable sample quantitation in our experiments. Moreover, upon incubating antibody-coated particles against an antigen sample, the peak area for the particle zone was seen to scale linearly with the antigen concentration establishing the utility of the reported focusing phenomenon for chemical/biochemical analysis. The noted stacking technique was further applied to also enabling UV absorbance detection of particle zones on microchips which yielded absorbance detection limits for 1 μm diameter preconcentrated polystyrene beads in a 5 µm deep quartz channel comparable to that measured for the same sample in a 300 µm inner diameter quartz capillary without any particle stacking.

2. Experimental Procedure

Device fabrication: For fabricating the microfluidic devices employed in this work, bottom substrates and cover plates made from borosilicate glass or quartz were purchased from Telic Company (Valencia, CA). While the purchased cover plates had both their faces unprotected, the bottom substrates came with a thin layer of chromium and photoresist laid down on one of their surfaces. Custom designed photomasks created through Fineline Imaging Inc. (Colorado Springs, CO) were used to pattern the desired channel layout onto the bottom substrate using standard photolithographic methods [29,30]. A simple cross-channel network was used in our experiments with all of its segments being 200 µm wide and uniformly deep (see Fig. 1). The length of the analysis channel in our device (segment D) was chosen to be 3.5 cm. After completion of the photo-patterning process, the photoresist layer was cured in microposit developer MF-319 (Rohm and Haas) and the chromium layer removed along the channel network with a chromium etchant (Transene Inc.). The fluidic ducts were then etched to depths between 2.5 and 30 µm, using a buffered oxide etchant (Transene Inc.). The protective photoresist and chromium layers on the bottom substrate were subsequently removed using the MF-319 and chromium etchant solutions, respectively. Access holes were drilled at the channel terminals using a microabrasive powder blasting system (Vaniman Inc.) to allow the introduction of liquid reagents/ samples into the microchannels. Finally, the microfluidic network was sealed off by bringing a glass cover plate in contact with the bottom substrate in deionized water and allowing the two plates to bond at 550°C for 9 h [31]. Cylindrical glass reservoirs with internal volumes of about 150 μL were affixed over the access holes using a ultraviolet light curable glue (Norland Products Inc.) to serve as a source or sink for the liquid flow within the microchannels.

Device operation: The reported microchip was prepared for an experiment by rinsing the entire fluidic network with 0.1 M sodium hydroxide followed by deionized water and the appropriate continuous phase for 20 min each. Particle injection into the analysis channel (segment D) was accomplished by placing the

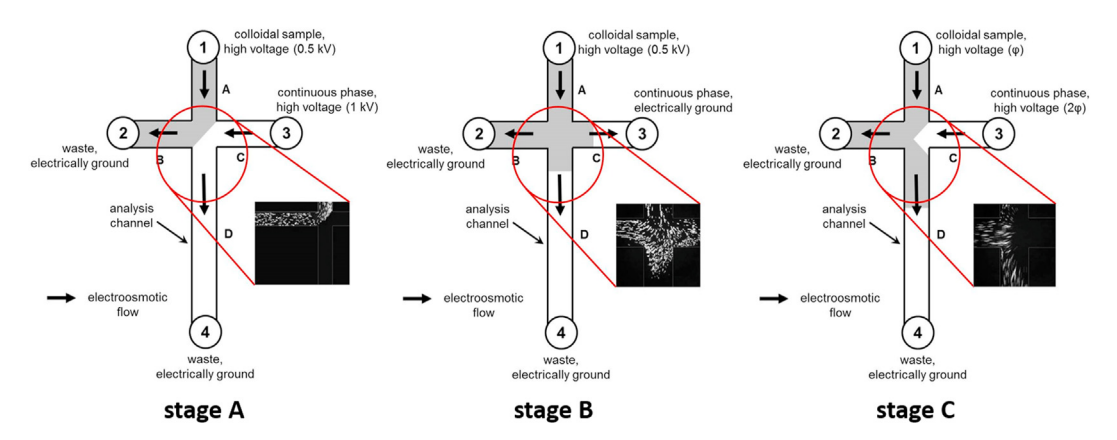


Fig. 1. Electrokinetic introduction of a particle band into the analysis channel using the gated injection scheme in the cross-channel layout used in our current work. The fluorescence images presented above were obtained using a 0.1 wt% solution of 1 μ m diameter fluorescently labeled polystyrene beads suspended in deionized water. A microchip with 5 μ m deep channel segments was used in this experiment operated at a voltage of $\phi = 1000 \, V$.

colloidal suspension of polystyrene beads (Thermo Fisher Scientific Inc.) in reservoir 1 while filling the remaining reservoirs with the corresponding continuous phase. The application of high voltages to reservoirs 1 and 3 (0.5 kV and 1 kV, respectively) under these conditions while electrically grounding reservoirs 2 and 4 then allowed the realization of a particle flow profile that was suitable for band injection (see Fig. 1, stage A). In order to introduce the particle bands into segment D of our device, a gated injection scheme was used [32]. This scheme was implemented by electrically grounding reservoir 3 for 0.5–8 s during which the particles were allowed to fill up the entire injection cross (see Fig. 1, stage B). This period spanning stage B has been referred to as the injection time (τ_{ini}) in the present work. Following this step, the electric potentials at reservoirs 1 and 3 were switched back to the operation voltages (ϕ and 2ϕ , respectively) to be used in the experiment, which also forced a fraction of the particles that had filled up the injection cross to be swept into segment D (see Fig. 1, stage C). Notice that the voltage applied at terminal 3 was always chosen to be 2 times the voltage applied to terminal 1 in all stages of our microchip operation, as it yielded a clean injection of the particle band into the analysis channel. The particle bands thus injected into segment D were detected at various distances downstream of the injection cross via the laser induced fluorescence (LIF) or UV absorbance techniques. For the LIF measurements, a laser beam (125 mW Argon ion tunable laser, Melles Griot) of wavelength 488 nm was used to excite the fluorophores on the beads and the resulting fluorescence signal collected using a photomultiplier tube (PMT) purchased from Hamamatsu Photonics after passing it through an appropriate (514 nm longpass) optical filter (Semrock Inc.). In experiments involving the UV absorbance detection of the polystyrene beads, a commercially available 260 nm deep UV LED (UVTOP255-BL-TO39) from Roithner Lasertechnik (Vienna, Austria) was used as the light source. The LED light was stacked onto the microchip/capillary using a 3 mm diameter fused silica ball lens (Edmund Optics) after passing it through a 260 \pm 20 nm bandpass optical filter (Semrock Inc.). The same PMT detector as noted above was used for the absorbance measurements but now placed along the path of the incident beam. The microchip and capillaries (Hampton Research) used in the absorbance measurements were made from quartz. The sequence of voltages applied to the different microchannel terminals during the sample injection/preconcentration stages and the data acquisition process by the photomultiplier tube were controlled using a LABVIEW program. The peak shapes were analyzed in our work with numerical data analysis tools available in MATLAB. The visualization of the fluorescent particle bands was realized in this study using an epifluorescence microscope (Nikon) with bandpass excitation (470–490 nm) and emission (520–560 nm) optical filters. The fluorescence images/videos of the migrating particle bands were recorded using a CCD camera (Roper Scientific) in this set-up. The absorbance measurements in the quartz capillaries were performed by simply filling up these conduits with the sample suspension of polystyrene particles. No sample injection was performed or electric field applied in these capillaries in order to prevent any pre-concentration effects.

Preparation of the polystyrene beads for measuring antigen concentrations: Streptavidin coated 1 µm diameter polystyrene beads were purchased (Nanocs Inc.) and suspended in a 1 mM sodium phosphate buffer (pH 7.4) to produce a 0.01 wt% colloidal solution. 400 µL of this solution was then aliquoted into a 1.5 mL microcentrifuge tube to which 20 µL of the biotinylated antibody solution (Mab1) to human TNF-α was added and incubated for 1 h after vortexing for 2 min. The biotinylated antibody purchased from Novus Biologicals was prepared in a 1 mM sodium phosphate buffer at a concentration of 5 µg/mL for this purpose. Following the incubation step, 1 mL of the 1 mM phosphate buffer was added to the tube and the mixture centrifuged for 30 min at 10.000 rpm. The centrifugation process allowed the beads to settle at the bottom of the assay tube. The supernatant solution was then removed from the tube without disturbing the beads. This washing step with the 1 mM phosphate buffer was repeated two more times to wash out the excess biotinylated antibodies. Later we introduced 20 µL of a human TNF-α sample (Millipore Sigma) prepared in the 1 mM phosphate buffer at various concentrations into the tube along with 400 μ L of additional buffer solution. After vortexing for 2 min, this solution was incubated for 1 h. Subsequently, the assay tube was washed with 1 mL solution of the buffer three times as described previously to rinse out the excess antigen. Subsequently, 400 μL of the buffer was added to the centrifuge tube along with a 20 μ L solution of 5 μ g/mL FITC tagged detection antibody (Mab11) to human TNF- α . The mixture was vortexed for 2 min and then incubated for an hour. The excess detection antibody solution was later washed out using three rinses with the 1 mL phosphate buffer as described previously, and the beads finally suspended in a 500 µL phosphate buffer solution after vortexing for 2 min. This colloidal suspension was electrokinetically injected into the microchannel to then assess the TNF- α concentration the beads were incubated against.

3. Results and discussion

Pre-concentration dynamics: The dynamics of the particle preconcentration process reported in this manuscript was investigated by visualizing the electrokinetic migration of fluorescent particle bands through the analysis channel. In Fig. 2, we have presented fluorescence images from these visualization experiments which show the noted pre-concentration process to begin with the creation a small stacked region of particles near the tail end of the injected band. This region is then noticed to electrokinetically migrate faster than the rest of the zone causing particles traveling in front to merge into it leading to the reported stacking effect. Videos of a migrating particle band as recorded at various distances downstream of the injection cross have been included as Supplemental Material to this manuscript to better illustrate this process. The images/videos noted above further show that as the stacked region of beads migrates through the fluidic conduit, it also constantly loses particles from its rear end. In the initial stages of the pre-concentration process the rate at which this region stacks up particles on its front side however, significantly exceeds the amount of beads lost from its tail end. Consequently, the stacked region is observed to grow in size and concentration with time eventually running out of particles that can be stacked at its leading edge. At this point, particle loss from the tail end of the band causes the stacked zone to slowly disintegrate leading to the eventual decay in the fluorescence signal shown in Fig. 2. The extent of particle stacking realized in our experiments has been quantitated using a pre-concentration factor, f, defined as $f = (I - I_b)/(I_0 - I_b)$. In this expression, I denotes the height of the sample peak recorded by the detector as the stacked particle band migrates through the analysis channel, whereas I_0 and I_b refer to the signals measured by our PMT upon entirely filling up this conduit with the corresponding colloidal suspension and continuous phase, respectively. The dynamics of the pre-concentration process as noted above can be captured in the magnitude of f measured at different distances downstream of the injection cross. For example, for a sample zone comprising 1 µm diameter polystyrene beads flowing through a 5 μ m deep channel, the quantity f is seen to attain a value of 83.6 about 1.5 cm downstream of the injection cross, i.e., L = 1.5 cm, substantially greater than its magnitude at L = 0.5 cm or 2.0 cm (see Fig. 2).

Effect of operating conditions: The pre-concentration phenomenon described in this article is strongly affected by the operating conditions chosen for the experiments, much of which have been captured in Figs. 3 and 4. For example, the variation in the preconcentration factor (f) with the migration distance in the analysis

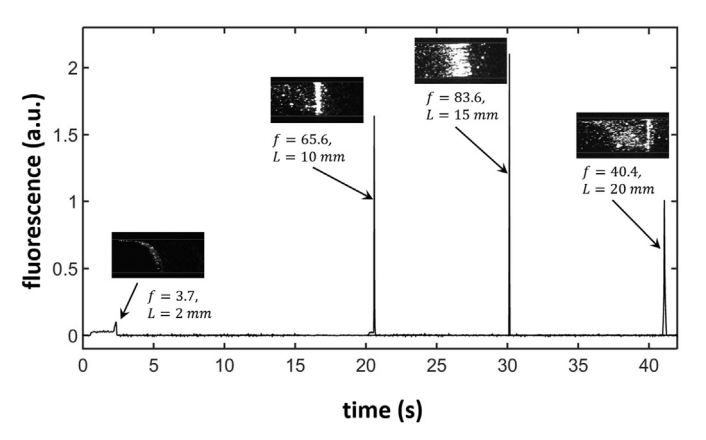


Fig. 2. Electrokinetic pre-concentration of a band of 1 μ m diameter polystyrene beads as it migrates through a 5 μ m deep glass channel for an operating voltage $\phi=1000$ V. The different peaks included in the figure were obtained by overlaying the electropherograms recorded at 2, 10, 15 and 20 mm downstream of the injection cross. A 0.02 wt% solution of fluorescent polystyrene beads suspended in deionized water was used in the experiments shown above for a choice of $\tau_{ini}=1$ s.

channel has been depicted in Fig. 3(a) which shows a maximum in the curve (f_{max}) as expected from the results included in Fig. 2. For 1 μm sized polystyrene beads being migrated through a 5 μm deep glass channel, this maximum occurs around L = 1.5 cm when $\phi =$ 1000 V. The figure further shows f_{max} to be highly sensitive to the particle size and is seen to attain its largest values for a particle diameter of 1 um indicating that both highly confining ducts as well as those offering little confinement to be non-optimal for the noted pre-concentration process. In Fig. 3(b), the effect of ϕ on particle stacking has been explored which shows f to again go through a maxima upon detecting the particles at a fixed migration distance (L = 1.5 cm) from the injection cross. This observation is a result of the particle zone being stacked more rapidly with increasing electric field strengths in segment D. Such reduction in the stacking time causes the polystyrene band to attain larger values of f at L=1.5 cm for all particle sizes at small electric field strengths. However, the noted trend is eventually reversed once the location at which *f* is maximized moves upstream of the detection point. The figure also shows the noted maximum value for f decreases in magnitude upon flowing the 1 µm diameter beads though increasingly deeper channels consistent with the results included in Fig. 3(a). To highlight the effect of particle confinement on the noted pre-concentration process, Fig. 4(a) presents some of the data points borrowed from Fig. 3(a) and 3(b) at L=1.5~cm and $\phi=$ 1250 V but now plotted against the ratio of the particle diameter to the channel depth which we denote by the symbol $\lambda = d_p/d$ in this analysis. The figure shows that for $\lambda < 0.1$, the quantity f is seen to exhibit a maximum (f_{max}) as d_p/d is increased attaining values as large as 114 in these measurements. Also, upon increasing the particle size (d_p) in the system, the value of λ at which f_{max} occurs is seen to increase but then diminishing the magnitude of f_{max} for relatively large bead sizes $d_p > 1 \mu m$. For the particle sizes chosen in this study, f_{max} was mostly attained when λ was in the range of 0.1-0.5. Nevertheless, the quantity f always went through a maximum irrespective of the choice for the particle diameter and channel depth in our experiments. We would like to point out that because the voltages applied to the channel terminals in stages A and B of microchip operation (see Fig. 1) were fixed in our experiments, we expected the sample volume introduced into segment D to be relatively constant for a given choice of the injection time (τ_{ini}) . Notice that the data included in Fig. 1 through 4(a) were all obtained for a choice of $\tau_{inj} = 1$ s. In Fig. 4(b), this parameter however was varied to see its effects on the pre-concentration factor as recorded at a fixed detection point (L = 1 or 2 cm). This study shows an improvement in the magnitude of f when τ_{ini} is increased to \sim 2 s for L=1 cm beyond which the pre-concentration factor does not change to any significant extent with increasing τ_{inj} . The noted behavior is observed as the particle zone attains f_{max} upstream of the detection point for τ_{inj} < 2 s and is therefore able to stack larger amounts of beads with increasing values of the injection time (and sample volume). Once τ_{inj} exceeds 2 s, the preconcentration factor is likely maximized downstream of the detection point and hence the extent of particle stacking realized at the location L = 1 cm remains unaffected by the sample volume injected into segment D. This hypothesis is also supported by the observation made further downstream, i.e., L = 2 cm, in which case the quantity f increased even for $\tau_{inj} > 2$ s but then tapered off beyond $\tau_{ini} = 4$ s. Moreover, the maximum value attained by f at L=2 cm was also substantially larger than that realized at L=1 cm again due to the greater amount of sample available for preconcentration in the former case. The data included in Fig. 4(b) also indicate that the extent of particle stacking is compromised when lower particle concentration or higher ionic strength buffers (in our case sodium phosphate buffer at pH 7.4) are used in the experiments. These observations suggest that particle-particle

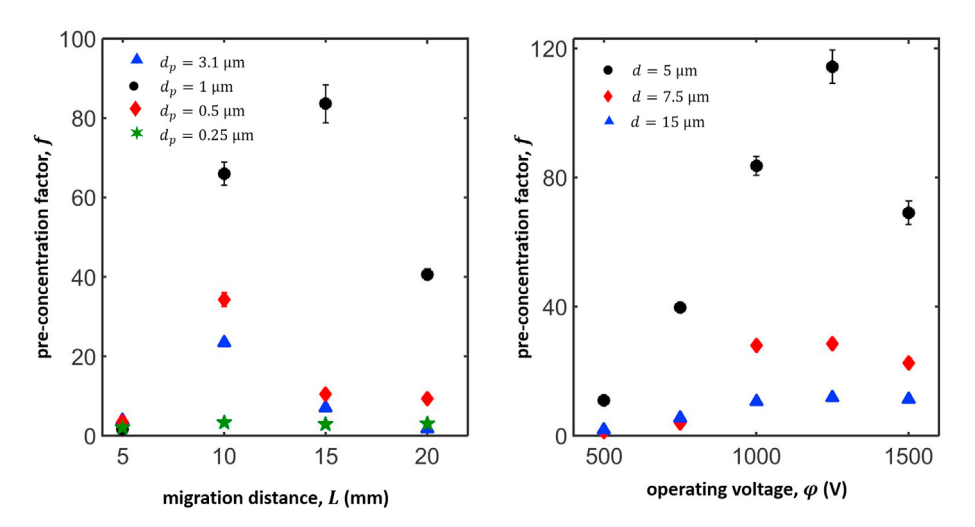


Fig. 3. (a) Extent of pre-concentration for the particle band as measured at different migration distance from the injection cross in a 5 μm deep channel. An operating voltage of $\phi = 1000$ V was used for these experiments. (b) Effect of operating voltage (ϕ) on the extent of pre-concentration for a band of 1 μm diameter polystyrene beads detected 1.5 cm downstream of the injection cross. For the experiments included in sub-figures (a) and (b), a sample containing 0.02 wt% polystyrene beads prepared in deionized water was used along with a choice of $\tau_{inj} = 1$ s. The error bars included in the figures are based on 5 measurements.

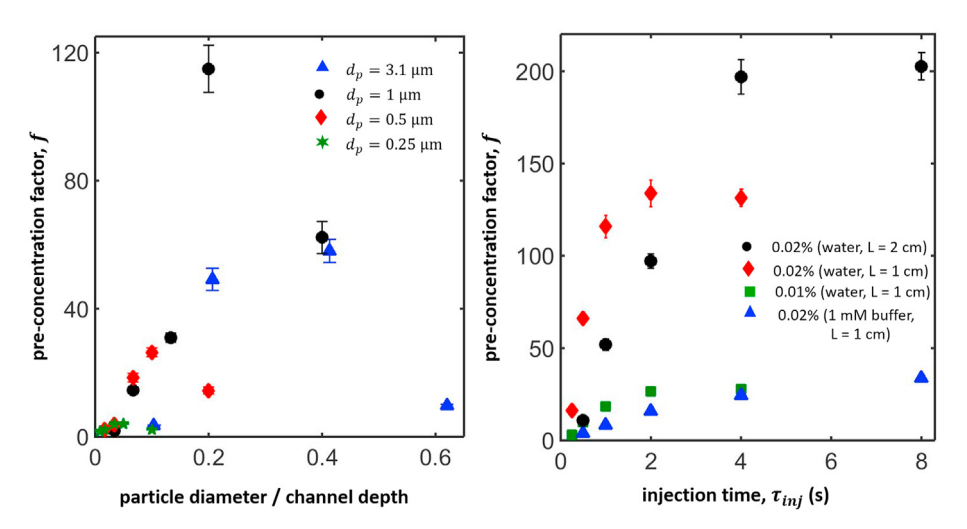


Fig. 4. (a) Effect of particle size and channel depth on the pre-concentration of 0.02 wt% polystyrene beads suspended in deionized water for an operating voltage of $\phi=1250\,\text{V}$. The particle zone was detected 1.5 cm downstream of the injection cross in these experiments for a choice of $\tau_{inj}=1\,\text{s}$. (b) Effect of injection time on the pre-concentration of 1 μm diameter polystyrene beads flowing through a 5 μm deep channel for a choice of $\phi=1250\,\text{V}$ and $L=1\,\text{or}\,2\,\text{cm}$. The numbers associated with the different symbols refers to the particle concentration used in the sample. The information included within the parenthesis next to these numbers indicate the continuous phase used in the sample and the location of the detection point in the measurement. The error bars included in all the figures are based on 5 measurements.

interactions may be playing an important role in the noted preconcentration process. Also, an increase in the ionic strength of the mobile phase slows down particle migration rates due to a decrease in the electroosmotic mobility of the continuous phase which previous experiments have indicated to have a negative impact on the stacking phenomenon. In addition, the mobile phase composition may also be influencing particle-particle interactions as well as contributing to electromigration effects [33,34] around the particle zone leading to the observations shown in Fig. 4(b). Nevertheless, we would like to point out that the reported preconcentration phenomenon was not substantially influenced by the electrical charge on the particles as similar values of f were recorded for both uncoated (marginally anionic according to the manufacturer) and amine coated (cationic) polystyrene beads when electrokinetically migrated through a glass channel under similar conditions (data not included). This observation suggests that electro-migration effects such as field amplified stacking may

only be contributing to the reported pre-concentration process in a minor way.

Sample quantitation approach: As has been noted previously, the particle stacking phenomenon described in this article is seen to exhibit a substantial variation in the height of the sample peak during its transit through the system. In this situation, we assessed the feasibility for sample quantitation based on the area under the analyte peak recorded by our detector. In Fig. 5(a), the peak area measured at different locations downstream of the injection cross for 1 μ m diameter polystyrene beads migrating through a 5 μ m deep channel has been presented which is seen to be relatively steady irrespective of the pre-concentration factor experienced by the sample zone. Moreover, this area is observed to decrease proportionally upon ramping up the operating voltage and therefore, the migration velocity of the particles in the system. Also, an increase in the injected sample volume by prolonging τ_{inj} was noticed to grow the peak area as expected in these measurements. Building on these

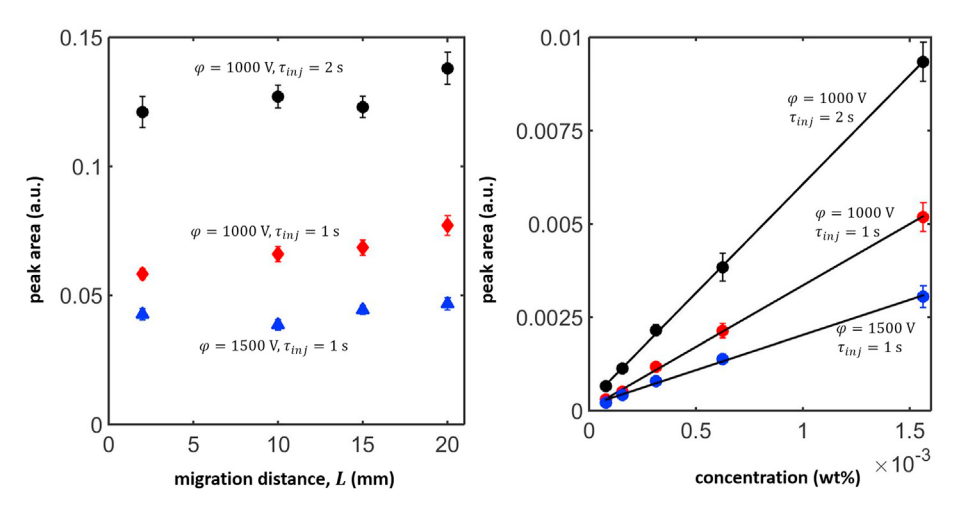


Fig. 5. (a) Area under the sample peak recorded by the detector at different locations downstream of the injection cross upon electrokinetically migrating a sample zone of 0.02 wt% polystyrene particles. Notice the proportional change in peak area upon altering the operating voltage (ϕ) and injection time (τ_{inj}) in the experiments. (b) Observed variation in peak area with particle concentration in the sample solution as recorded 15 mm downstream of the injection cross for different choices of ϕ and τ_{inj} . The data included in both figures were obtained by migrating 1 μm diameter fluorescent polystyrene particles through a 5 μm deep glass channel. These samples were prepared using deionized water as the continuous phase. The error bars included in both the figures are based on 5 measurements.

results, the variation in the peak area with particle concentration recorded 15 mm downstream of the injection cross was determined which yielded a linear relationship between the two quantities. The slope of the best fit line in these measurements was further seen to vary with the parameters ϕ and au_{inj} in an expected manner. Overall, the experiments described above clearly established the area under the sample peak as a reliable measure for sample quantitation in our system. We would like to mention that the data included in Fig. 5(b) yields a detection limit of about 6.4×10^{-5} wt% for the fluorescent polystyrene beads when they were electrokinetically migrated through a 5 µm deep channel employing $\phi = 1000 V$ and $\tau_{ini} = 1 s$. This translates to about a 95-fold improvement in the detectability of the particles compared to the situation when they were not preconcentrated in the 5 μm deep channel and yielded a detection limit of about 6.1×10^{-3} wt% in our experimental set-up. The detection limit in the above analysis was calculated as the sample particle concentration that yielded a signal-to-noise ratio of 3 in the relevant fluorescence measurements.

Integration to UV absorbance detection: While fluorescent labels enable sensitive detection of particles as is desirable in microfluidic channels with small optical path lengths, they are not ideal for characterizing these entities. This is because such labeling has a tendency to alter the chemical reactivity of the particles as well as modify their physical properties, e.g., zeta potential, refractive index, etc. In this situation, a label-free detection method for particulate matter is often preferred which is commonly accomplished based on the UV absorbance technique. The sensitivity of UV absorbance measurements however is limited, and only allows sample detection in systems with an optical path length of about a millimeter or more. As a result, this detection method is often not suitable for label-free detection of particles and other analytes in microfluidic channels which typically offer optical path lengths on the order of 10–100 μm. In this work, UV detection of polystyrene beads has been enabled through electrokinetic preconcentration of the particle zones as described in the previous sections. In Fig. 6(a), we have presented the recorded variation in the sample peak area with particle concentration for 1 μ m diameter non-fluorescent polystyrene beads which shows a linear trend between the two quantities similar to that observed for the fluorescence measurements. However, the signal-to-noise ratio in this case was significantly worse and yielded a detection limit of about 2.3×10^{-3} wt% upon electrokinetically pre-concentrating the particle zones in a 5 µm deep quartz channel for a choice $\phi=1000~V$ and $\tau_{inj}=1~s$. In the absence of any pre-concentration effects, this particle detection limit for the same measurement increased by about 87-folds to a value of 0.2 wt%. In addition to the noted microchip measurements, we also quantified UV absorbance based particle detection in a commercially fabricated 300 µm inner diameter quartz capillary without any pre-concentration effects for comparison purposes. As may be seen from Fig. 6(b), this study yielded a detection limit of about 2.1×10^{-3} wt% for the 1 µm diameter non-fluorescent polystyrene beads which is comparable to that obtained for the same sample in a 5 µm deep quartz channel upon electrokinetically pre-concentrating the particle zones applying $\phi=1000~V$ and $\tau_{inj}=1~s$.

Estimation of colloidal matter in natural water samples: The ability to detect colloidal particles in microchannels via the labelfree UV absorbance method broadens the kinds of liquid samples that may be analyzed using microfluidic systems. Natural water samples represent one such class of specimen that are known to contain varying amounts of colloidal matter depending on the environment in which they originate. We therefore demonstrated a real world application of our particle stacking method by employing it to assess the colloidal content of natural water samples collected from Laramie River in Laramie, Wyoming. Samples were collected from two different locations that were about 10 miles apart with the location for sample S1 being downstream to that of S2. The noted water samples were first filtrated through a syringe filter (Millipore Sigma) having a pore size of 1.2 µm. Different dilutions of these samples prepared in de-ionized water were then placed in reservoir 1 of our quartz microchip device while filling the remaining reservoirs with de-ionized water. To analyze them, the colloidal samples were electrokinetically injected into a 5 µm deep channel and the particle pre-concentration process realized by setting $\phi = 1000 V$ and $\tau_{ini} = 2$ s in our experiments. The pre-concentrated zones were subsequently detected 15 mm downstream of the injection cross using the UV absorbance system described in the previous section. The recorded peaks were quantitated in our analysis based on the area under the curve which was seen to correlate linearly with the reciprocal of the dilution factor for the samples (see Fig. 7(a)). Also, comparing the signal for the undiluted samples to the response curve for polystyrene beads included in Fig. 6(a) generated under the

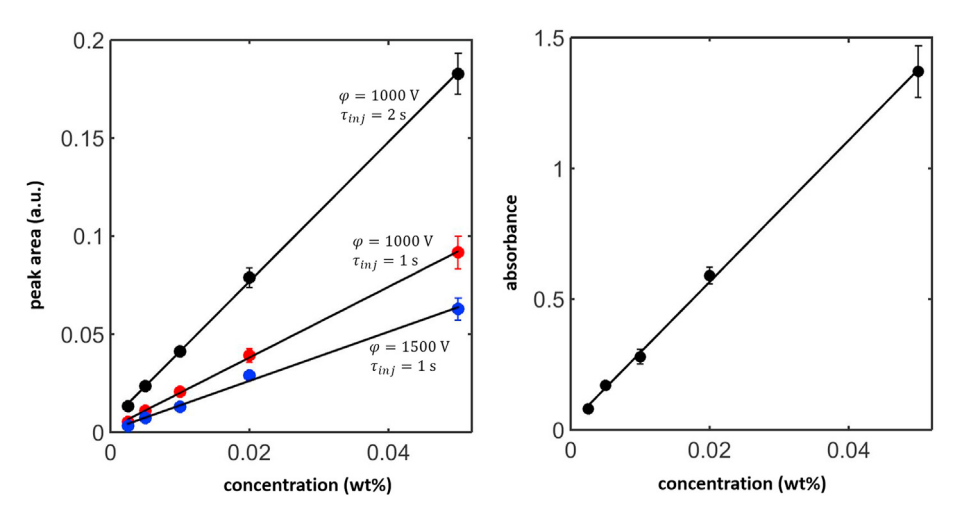


Fig. 6. (a) Observed variation in peak area with particle concentration measured in a 5 μm deep quartz channel based on the UV absorbance detection method. The sample peaks in these experiments were recorded 15 mm downstream of the injection cross for different choices of ϕ and τ_{inj} . (b) Observed variation in the UV absorbance with particle concentration as recorded upon filling a 300 μm inner diameter quartz capillary with the sample solution. The data included in both figures were obtained with 1 μm diameter non-fluorescent polystyrene particle samples using deionized water as the continuous phase. The error bars included in both the figures are based on 5 measurements.

conditions $\phi = 1000 \ V$ and $\tau_{inj} = 2 \ s$ indicate a colloidal content of 0.026 wt% and 0.019 wt% for samples S1 and S2. The validity of these estimated colloidal weight percentages were assessed by analyzing the natural water samples using a gravimetric method. In these gravimetric measurements, 10 mL of the natural water samples were first filtrated through a 1.2 µm syringe filter, and then weighed before and after passing it through a 0.45 µm syringe filter yielding 0.031 and 0.023 wt% of particulate matter in the S1 and S2 samples, respectively. It must be noted that the colloidal content in the S1 and S2 samples as estimated by the gravimetric technique was somewhat higher than that determined by our microfluidic particle preconcentration method. This may have occurred as the filtered natural water samples likely contained particles of varying sizes as compared to the polystyrene bead specimen used in our experiments which were relatively monodisperse. In this situation, any colloidal matter in our natural water samples that had linear dimensions significantly smaller than 1 um was likely not preconcentrated and detected. Moreover, the irregular shape, material (e.g., dielectric constant) and optical properties of the particles suspended in the tested natural water samples relative to that for the spherical polystyrene beads also likely contributed to the discrepancy in results obtained using the microfluidic and gravimetric approaches. Nevertheless, our microfluidic platform provided an excellent estimate for selectively determining the fraction of colloidal matter in the tested natural water samples with linear dimensions in the range of 10-25% of the chosen channel depth $(5~\mu m)$.

Antigen concentration measurements: In order to establish the utility of the reported particle stacking technique for chemical and biochemical analysis, we also applied it to estimating antigen concentrations in liquid samples upon incubating antibody-coated polystyrene beads against such samples. For these experiments, the relevant colloidal suspensions prepared by following the steps described in the "Experimental Procedure" section were electrokinetically injected into a 5 μ m deep channel and the particle preconcentration process realized by setting $\phi=1000~V$ and $\tau_{inj}=2~s$. The pre-concentrated particle zones were subsequently detected 15 mm downstream of the injection cross using the LIF detection

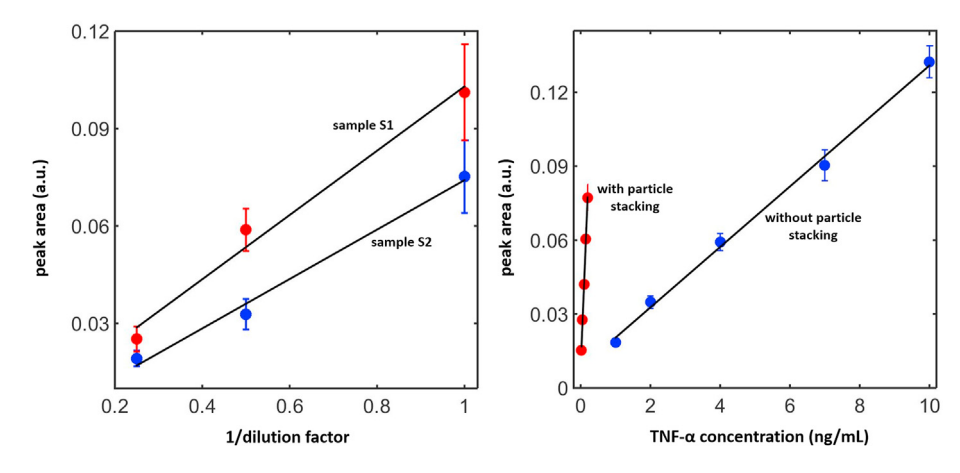


Fig. 7. (a) Observed variation in peak area with the reciprocal of the dilution factor for the tested natural water samples S1 and S2 measured in a 5 μ m deep quartz channel based on the UV absorbance detection method. The sample peaks in these experiments were recorded 15 mm downstream of the injection cross setting $\phi = 1000 \, V$ and $\tau_{inj} = 2s$. (b) Recorded variation in peak area with the concentration of human TNF- α incubated against the 1 μ m diameter antibody-coated polystyrene beads when migrated through a 5 μ m deep glass channel. The sample peaks in these experiments were recorded 15 mm downstream of the injection cross setting $\phi = 1000 \, V$ and $\tau_{inj} = 2s$. The error bars included in both the figures are based on 5 measurements.

set-up described previously. The recorded peaks were quantitated in our analysis based on the area under the curve which was seen to correlate linearly with the human TNF- α (antigen) concentration, the beads were incubated against (see Fig. 7(b)). Based on this response curve, the detection limit for TNF- α was determined to be about 31 pg/mL which was nearly 29-fold lower than that recorded in the same 5 μ m deep glass channel without any particle stacking effects. These results establish the utility of the reported particle pre-concentration technique for assessing liquid sample compositions in a variety chemical/biochemical assays commonly employed in research and diagnostic applications.

4. Conclusions

To summarize, we report a novel pre-concentration phenomenon for micro- and nanoparticle bands during their electroosmotic migration through a glass channel of uniform cross-section. Preconcentration factors over 2 orders of magnitude were recorded based on this process with the strongest stacking effect occurring for high electroosmotic flow velocities and particle diameter to channel depth ratios in the range of 0.2-0.4. Visualization experiments suggest the reported stacking process to be initiating at the tail end of the particle zone during its electrokinetic injection into the analysis channel with the stacked region migrating faster than the rest of the cluster collecting more particles at its upstream end. However, once the pre-concentrated zone runs out of particles at its front end, it disintegrates slowly due to loss of particles from its tail end. While the exact details for the noted particle stacking process is unclear, it is likely a result of a complex interplay of electrokinetic and hydrodynamic forces in the system which may be deciphered through careful simulation of particle transport in shallow microchannels. Nevertheless, this experimental report offers some useful information towards understanding the noted pre-concentration phenomenon and lays down a solid foundation for future theoretical/numerical investigations on the topic. While the dynamics of the particle pre-concentration process noted above leads to a temporal variation in the height of the sample peak recorded by the detector, the area under this peak is observed to remain relatively constant allowing reliable sample quantitation. In the present work, the noted stacking technique was further applied to enabling UV absorbance detection of particle zones on microchips which then allowed us to determine the colloidal content in actual natural water samples. Our estimates of this colloidal content employing the reported particle pre-concentration phenomenon compared well with independent measurements made on the same samples using a gravimetric method. Finally, it was also demonstrated that upon incubating antibody-coated particles against an antigen sample, the peak area for the particle zone scaled linearly with the antigen concentration establishing the utility of the reported focusing phenomenon for a variety of chemical/biochemical analysis. Interestingly, the electrokinetic focusing phenomenon reported in this article has been recently observed to also narrow down zones of DNA samples. The authors are currently characterizing this DNA focusing effect and expect to publish their findings in a future manuscript.

CRediT authorship contribution statement

Ling Xia: Experimentation, Visualization, Methodology, development, Data curation, Formal analysis, data collection, Formal analysis. **Rajesh Deb:** Experimentation, Visualization, Methodology, development, Data curation, Formal anlysis, data collection,

Formal analysis, Validation. **Debashis Dutta:** Conceptualization, Methodology, collection, Data curation, Formal analysis, Formal analysis, Writing - original draft, Writing - review & editing, Supervision, Project administration, Funding acquisition.

Declaration of competing interest

The authors declare that they have no known competing financial interests or personal relationships that could have appeared to influence the work reported in this paper.

Acknowledgements

DD acknowledges funds from the National Science Foundation (CHE 1808507) and the National Institutes of Health (1R15AG045755-01A1) for carrying out the experiments included in this manuscript. RD also acknowledges graduate assistantship through the NIH-Wyoming INBRE program (P20GM103432).

Appendix A. Supplementary data

Supplementary data to this article can be found online at https://doi.org/10.1016/j.aca.2020.08.019.

References

- [1] P.A. Auroux, D. lossifidis, D.R. Reyes, A. Manz, Anal. Chem. 67 (2002) 2637–2652.
- [2] D.J. Beebe, G.A. Mensing, G.M. Walker, Annu. Rev. Biomed. Eng. 4 (2002) 261–286.
- [3] S. Haeberle, R. Zengerle, Lab Chip 7 (2007) 1094-1110.
- [4] W. Sparreboom, A. van den Berg, J.C.T. Eijkel, Nat. Nanotechnol. 4 (2009) 713–720.
- [5] M.L. Kovarik, S.C. Jacobson, Anal. Chem. 81 (2009) 7133-7140.
- [6] C.C. Lin, J.L. Hsu, G.B. Lee, Microfluid. Nanofluidics 10 (2011) 481-511.
- [7] B.C. Giordano, D.S. Burgi, S.J. Hart, A. Terray, Anal. Chim. Acta 718 (2012) 11–24.
- [8] M.C. Breadmore, A. Wuethrich, F. Li, S.C. Phung, U. Kalsoom, J.M. Cabot, M. Tehranirokh, A.I. Shallan, A.S. Abdul Keyon, H.H. See, M. Dawod, J.P. Quirino, Electrophoresis 38 (2017) 33–59.
- [9] J. Hu, S.Q. Wang, L. Wang, B.P. Murphy, T.J. Lu, F. Xu, Biosens. Bioelectron. 54 (2014) 585–597.
- [10] Y. Xia, J. Si, Z. Li, Biosens. Bioelectron. 77 (2016) 774–789.
- [11] A.V. Hatch, A.E. Herr, D.J. Throckmorton, J.S. Brennan, A.K. Singh, Anal. Chem. 78 (2006) 4976–4984.
- [12] R.S. Foote, J. Khandurina, S.C. Jacobson, J.M. Ramsey, Anal. Chem. 77 (2005) 57–63.
- [13] N. Yanagisawa, D. Dutta, Anal. Chem. 84 (2012) 7029-7036.
- [14] Y. Cong, S. Katipamula, T. Geng, S.A. Prost, K. Tang, R.T. Kelly, Electrophoresis 37 (2016) 455–462.
- [15] Y.C. Wang, A.L. Stevens, J.Y. Han, Anal. Chem. 77 (2005) 4293-4299.
- [16] J.Y. Han, J.P. Hu, R.B. Schoch, Lab Chip 8 (2008) 23–33.
- [17] B. Jung, R. Bharadwaj, J.G. Santiago, Anal. Chem. 78 (2006) 2319–2327.
- [18] B. Giri, D. Dutta, Anal. Chim. Acta 810 (2014) 32–38.
- [19] N. Beyor, T.S. Seo, P. Liu, R.A. Mathies, Biomed. Microdevices 10 (2008) 909–917.
- [20] H. Chen, Q. Fang, X.F. Yin, Z.L. Fang, Lab Chip 5 (2005) 719-725.
- [21] J. Voldman, Annu. Rev. Biomed. Eng. 8 (2006) 425–454.
- [22] Y.J. Kang, D.Q. Li, Microfluid. Nanofluidics 6 (2009) 431–460.
- [23] R. Pethig, Biomicrofluidics 4 (2010) article no: 022811.
- [24] B. Cetin, D. Li, Electrophoresis 30 (2009) 3124–3133.
 [25] Y. Solomentsev, M. Böhmer, J.L. Anderson, Langmuir 13 (1997) 6058–6068.
- [26] K.H. Bhatt, S. Gregio, O.D. Velev, Langmuir 21 (2005) 6603–6612.
- [27] W.D. Ristenpart, I.A. Aksay, D.A. Saville, J. Fluid Mech. 575 (2007) 83–109.
- [28] F. Zhang, D.Q. Li, J. Colloid Interface Sci. 410 (2013) 102-110.
- [29] D.C.S. Bien, P.V. Rainey, S.J.N. Mitchell, H.S. Gamble, J. Micromech. Microeng. 13 (2003) S34–S40.
- [30] G.M. Toh, N. Yanagisawa, R.C. Corcoran, D. Dutta, Microfluid. Nanofluidics 9 (2010) 1135–1141.
- [31] S.C. Jacobson, A.W. Moore, J.M. Ramsey, Anal. Chem. 67 (1995) 2059–2063.
- [32] S.V. Ermakov, S.C. Jacobson, J.M. Ramsey, Anal. Chem. 72 (2000) 3512–3517.
- [33] G.L. Erny, E.T. Bergström, D.M. Goodall, J. Chromatogr. A 959 (2002) 229–239.
- [34] Z. Chen, S. Ghosal, Bull. Math. Biol. 74 (2012) 346–355.